Dynamical behavior of the motions associated with the nonlinear periodic regime in a laboratory plasma subject to delayed feedback

T. Fukuyama,[1,*] Y. Watanabe,[3] K. Taniguchi,[2] H. Shirahama,[1] and Y. Kawai[3]
[1]*Faculty of Education, Ehime University, Bunkyo-cho 3, Matsuyama, Ehime 790-8577, Japan*
[2]*Department of Physics, Kyoto University of Education, Fujinomori-cho 1, Fukakusa, Fushimi-ku, Kyoto 612-8522, Japan*
[3]*Interdisciplinary Graduate School of Engineering Sciences, Kyushu University, Kasugakoen 6-1, Kasuga, Fukuoka 816-8580, Japan*
(Received 11 January 2006; published 6 July 2006)

Time-delayed feedback is applied to the motions associated with the nonlinear periodic regime generated due to current-driven ion acoustic instability; this is a typical instability in a laboratory plasma, and the dynamical behavior is experimentally investigated using delayed feedback. A time-delayed autosynchronization method is applied. When delayed feedback is applied to the nonlinear periodic orbit, the periodic state changes to various motions depending on the control parameters, namely, the arbitrary time delay and the proportionality constant. Lyapunov exponents are calculated in order to examine the dynamical behavior.

DOI: 10.1103/PhysRevE.74.016401 PACS number(s): 52.35.Mw, 05.45.Gg

I. INTRODUCTION

In dissipative physical systems, such as those that occur in plasmas, fluids, lasers, etc., it is often observed that the system is described by a state of sustained chaotic motion. Furthermore, the problem of controlling chaos has recently attracted great interest [1–6]. In particular, time-delayed feedback [2] plays a prominent role in controlling chaos; this is one of the successful applications that knowledge acquired in nonlinear science has provided to plasma physics beyond its own specialized area of study. Currently, applications such as controlling chaos have attracted considerable attention in plasma physics for understanding "turbulence." The crucial role of turbulence in fusion-oriented plasmas has led to a special interest in controlling chaos. Turbulence is often a problematic phenomenon that may have harmful consequences. Chaos in high density and magnetized plasmas such as fusion-oriented plasmas, which requires stabilization, will evolve into a fully developed turbulence. Several systems reach turbulence via chaos. Therefore, the investigation of chaos control should contribute to understanding plasma turbulence.

There are some methods of controlling chaos wherein the main idea is to convert chaotic behavior to periodic behavior by inducing a small perturbation in the system. Time-delayed feedback is frequently used as an effective method of controlling chaos. Pyragas [2] has proposed the time-delayed feedback technique, which is based on feedback perturbation in the form of the difference between a delayed output signal and the output signal itself; this is appropriate for laboratory experiments conducted in real time. This method is robust to noise and does not require real-time computer processing to calculate a target unstable periodic orbit (UPO); therefore, it can act on the experimental system continuously over time. The feedback perturbation signal $F(t)$ that is applied to the nonlinear system is proportionally adjusted to the difference between the two successive values of an arbitrary dynamic variable $x(t)$, $F(t)=k[x(t-\tau)-x(t)]$. Here, τ is the time delay, which agrees with the period of a UPO embedded in the chaotic attractor while controlling chaos, and k is its proportionality constant. Since a plasma is a typical nonlinear dynamical system with a large number of degrees of spatiotemporal freedom, various unexpected phenomena are observed when time-delayed feedback is applied in a plasma. A system in which the time-delayed feedback is applied has infinite dimensions; therefore, τ and k should be carefully selected while controlling chaos. Recently, control of chaos generated due to the current-driven ion acoustic instability (IAI) has been reported [7–9]. It has been reported that chaos can be effectively controlled by using the time-delayed feedback method. In this study, delayed feedback is applied to the motions associated with the nonlinear periodic regime (NPR) before it develops chaotic motion. This is because the range of a nonlinear periodic orbit can be attributed to a wide variety of physical mechanisms. When information propagates, spatially extended systems such as plasmas and fluids themselves have a time delay. The occurrence of the time delay is an unavoidable problem with regard to controlling chaos. Therefore, investigations into the behavior of nonlinear systems with regard to time delay are currently required.

In this paper, the dynamical behavior in a laboratory plasma is reported in detail in this regard. In Sec. II, the experimental setup is described. In Sec. III, the behavior of the system is described on changing τ and k when time-delayed feedback is applied to the motions associated with the NPR. Lyapunov exponents are shown in order to examine the dynamical behavior with the time-delayed feedback. In Sec. IV, the findings are summarized.

II. EXPERIMENTAL SETUP

The experiments are performed using a double-plasma device [10] with a diameter of 70 cm and a length of 120 cm. The chamber of the device contains two cages made of multipole permanent magnets for surface plasma confinement; they also have tungsten filaments around the chamber wall that act as cathodes. The chamber is divided at the center into a driver region and a target region by a separation grid that is kept at a floating potential. In this experiment, the plasma is

*Electronic address: fukuyama@ed.ehime-u.ac.jp

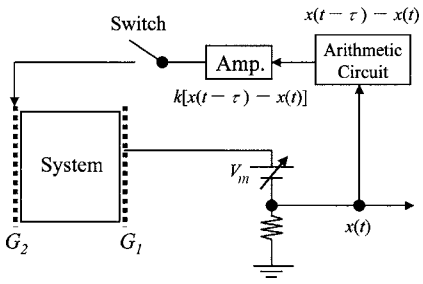

FIG. 1. Schematic representation of the experimental setup. Time series signals $x(t)$ for analysis are obtained from the fluctuating components of currents on the biased mesh grids.

generated only in the target region, which is the experimental region. The chamber is evacuated to 4.0×10^{-7} Torr, and argon gas is then introduced into the chamber at a pressure of 4.0×10^{-4} Torr. Typical plasma parameters are as follows: electron density $n_e\sim10^8$ cm^{-3}; and electron and ion temperatures $T_e\sim0.5-1.0$ eV and $T_i\sim T_e/(10-15)$, respectively. The current-driven IAI is excited by two parallel mesh grids G_1 and G_2 with the following dimensions: diameter 6 cm; grid 50 mesh/in.; and interval L 2.5 cm [11]. A dc potential V_m is applied to G_1 in order to excite the instability, and G_2 is kept at a floating potential. For analysis, time series signals $x(t)$ are obtained from the fluctuating components of the currents on the V_m-biased mesh grids, and the signals are sampled using a digital oscilloscope. In order to incorporate a time delay in the experiments, the feedback signal $F(x)$ is applied to the floating mesh grid G_2; this gives rise to a perturbation in the system. The feedback signal $F(x)$ is generated from $x(t)$ by using an electronic circuit based on the time-delayed feedback method. The experimental setup is schematically shown in Fig. 1.

III. RESULTS AND DISCUSSION

A. Current-driven ion acoustic instability

The current-driven IAI is caused by the interaction between electron streaming, i.e., the electron current, and the background ion acoustic waves in the plasma [12–17]. When V_m is applied to G_1 and G_2 is kept at floating potential, an electric field is obviously applied between the two mesh grids. The electrons are accelerated from G_1 toward G_2 by the applied electric field and the electron current flows between the two mesh grids. The current-driven IAI occurs due to the interaction between this electron current and the background ion acoustic wave in the plasma. When the grid potential V_m exceeds a threshold, a current-driven IAI is excited [8,9,11]. The behavior of the system as a function of the control parameter V_m is illustrated in Fig. 2, which shows the time series signal $x(t)$. Here, the sampling time Δt is 1.0×10^{-6} s. The instability, including burst waves, appears for $23\leqslant V_m\leqslant66$ V. When the instability grows, the waves become turbulent. When V_m exceeds 23 V, which corresponds to the threshold, a limit cycle appears and persists for $23\leqslant V_m\leqslant35$ V, as shown in Fig. 2(b). The amplitude of the limit cycle switches stochastically between two values for

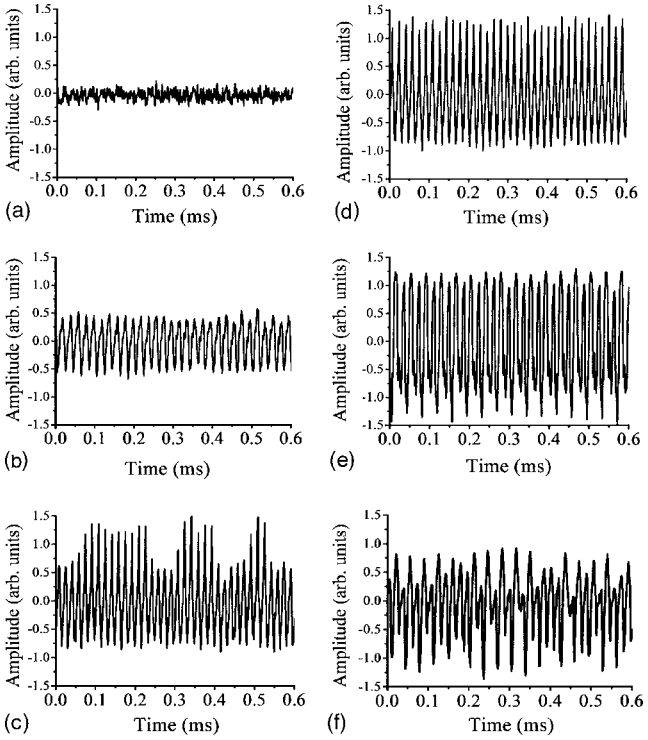

FIG. 2. Behavior of the system as a function of the control parameter V_m: (a) before excitation of instability (V_m=23 V), (b) a smaller limit cycle oscillation (V_m=26 V), (c) stochastic oscillation between two values (V_m=38 V), (d) a larger limit cycle oscillation (V_m=40 V), (e) chaos (V_m=47 V), and (f) chaos when the system is completely disturbed (V_m=54 V). The time series signals $x(t)$ are illustrated.

$36\leqslant V_m\leqslant39$ V, as shown in Fig. 2(c), and a larger limit cycle appears for $40\leqslant V_m\leqslant45$ V, as shown in Fig. 2(d). Subsequently, as V_m increases, the system gradually falls into disorder. Figures 2(e) and 2(f) show the chaotic state (V_m=47 V) and the typical chaotic state when the system is completely disturbed (V_m=54 V), respectively. When $V_m\geqslant67$ V, the instability disappears with a decrease in the noise level. In previous work [9], it has been reported that the chaotic state caused by the current-driven IAI is effectively controlled when time-delayed feedback is applied to a typical chaotic state, and control is achieved when the time delay is chosen near the particular period of the UPO approximately corresponding to the fundamental mode of the chaotic system. In this study, delayed feedback is applied to the motions associated with the NPR and its dynamical behavior is shown. Here, the system has a nonlinear periodic orbit when $40\leqslant V_m\leqslant45$ V—corresponding to Fig. 2(d)—before exhibiting chaotic motion. A nonlinear periodic orbit with delayed feedback can be attributed to a wide variety of physical mechanisms [18–20]. Time-delayed feedback is applied to the motions associated with the NPR when the parameter V_m is 40 V.

B. Experimental results

Figure 3 shows the behavior of the system versus the time delay τ. The proportionality constant k is fixed at 2.06. Left

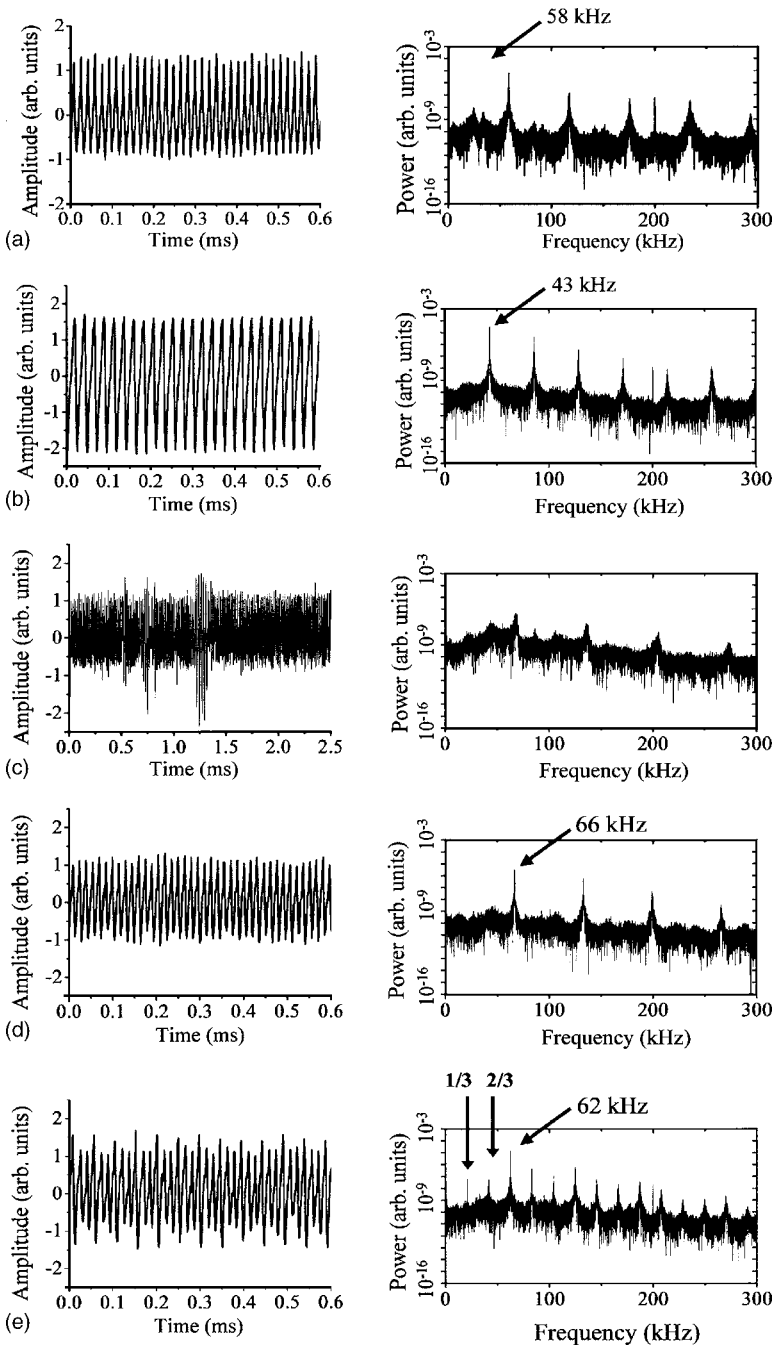

FIG. 3. Behavior of the system versus time delay τ. The proportionality constant k is fixed at 2.06. Left and right traces correspond to the time series signal $x(t)$ and power spectra, respectively. (a) Before application, (b) $\tau=11.25$ μs, (c) $\tau=13.75$ μs, (d) $\tau=15.0$ μs, and (e) $\tau=17.5$ μs.

and right traces correspond to the time series signal $x(t)$ and power spectra, respectively. Figure 3(a) shows the state of the system before the application of the time-delayed feedback, which corresponds to Fig. 2(d). After the application, the behavior of the system is investigated by changing τ. Figure 3(b) shows the state when $\tau=11.25$ μs ($\sim$0.65 period). Here, the fundamental frequency shifts to 2/3 the value of the peak of the system before the application of the time-delayed feedback. As τ increases, the system passes through an intermittent phase as shown in Fig. 3(c), and it exhibits periodic oscillation with another fundamental frequency, as shown in Fig. 3(d). This figure shows the state when $\tau=15.0$ μs ($\sim$0.87 period). Here, the frequency approaches the fundamental frequency before the application of the time-delayed feedback, which is determined by the boundary condition between the two mesh grids. It is shown that synchronization occurs when the time delay is chosen near the particular period that corresponds to the fundamental mode of the system before the time-delayed feedback is applied. Two limit cycles coexist in Fig. 3(c) because the limit cycle at 43 kHz gradually changes to the one at 66 kHz. Figure 3(c) shows the state when $\tau=13.75$ μs ($\sim$0.8 period). Since it oscillates between two regular states, the system has an intermittent feature as shown in Fig. 3(c). On further increasing τ, the system settles into an unstable period-3 orbit, as shown in Fig. 3(e). The figure shows the state when $\tau=17.5$ μs ($\sim$1.02 period). The time delay τ and proportionality constant k are not known *a priori*, and their appropriate

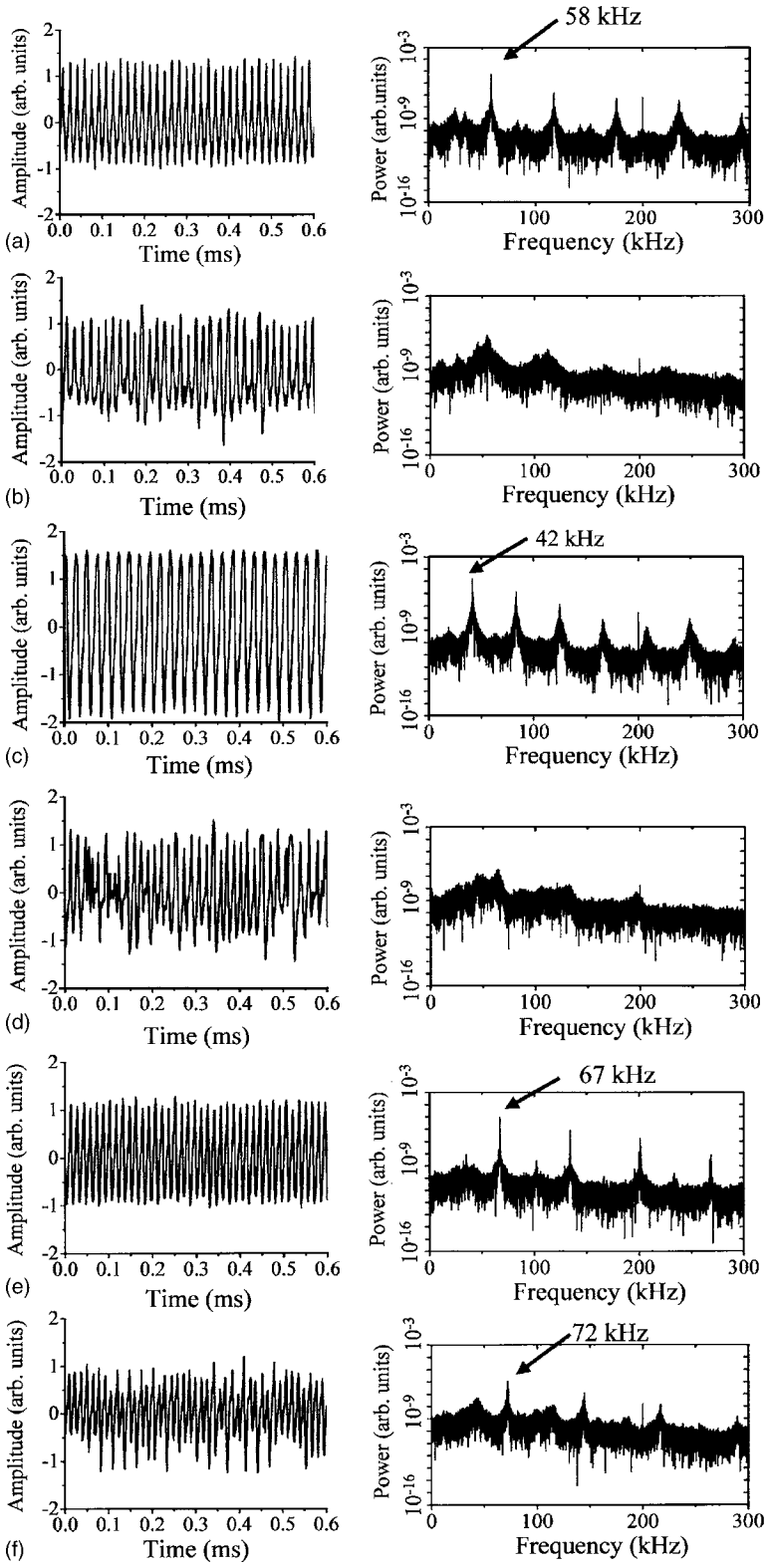

FIG. 4. Behavior of the system versus proportionality constant k. The time delay τ is fixed at 13.75 μs. Left and right traces correspond to the time series signal $x(t)$ and power spectra, respectively. (a) Before application, (b) $k=0.64$, (c) $k=0.86$, (d) $k=1.30$, (e) $k=1.48$, and (f) $k=3.0$.

values are determined by trial and error. Thus far, it has been experimentally demonstrated that synchronization is achieved only when τ is chosen near the particular period that corresponds to the fundamental mode of the original system. However, it is also observed that the system is synchronized when τ is selected as 11.25 μs, which corresponds to 2/3 the value of the peak of the system before the application of the time-delayed feedback, and the intensity of the peak is considerably low as compared to the fundamental one. Stabilization is achieved when a feedback signal is applied at a subharmonic frequency.

Figure 4 shows the behavior of the system versus the proportionality constant k. The time delay τ is fixed at 13.75 μs. The left and right traces correspond to the time

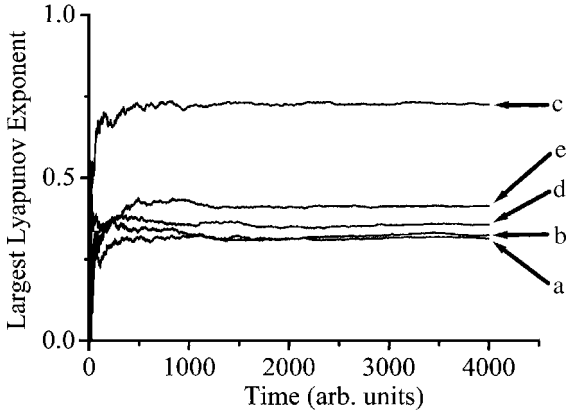

FIG. 5. The largest Lyapunov exponents calculated from the time series in Fig. 3. (a) 0.31 (before application), (b) 0.33 (τ=11.25 μs), (c) 0.73 (τ=13.75 μs), (d) 0.36 (τ=15.0 μs), and (e) 0.42 (τ=17.5 μs).

series signal $x(t)$ and power spectra, respectively. Figure 4(a) shows the state of the system before the application of the time-delayed feedback, which corresponds to Fig. 2(d). After the application, the behavior of the system is investigated by changing k. For $0.05 \leqslant k \leqslant 0.85$, the system exhibits a chaotic feature. Figure 4(b) shows the state when k=0.64. For $0.85 \leqslant k \leqslant 1.14$, the system shows a periodic oscillation. Figure 4(c) shows the state when k=0.86. Here, the fundamental frequency shifts to 2/3 the value of the peak of the system before the application of the time-delayed feedback. For $1.14 \leqslant k \leqslant 1.48$, the system exhibits a chaotic feature. Figure 4(d) shows the state when k=1.30. Chaotic oscillation is suppressed gradually as k increases. For $1.48 \leqslant k \leqslant 2.10$, the system again shows periodic oscillation. Figure 4(e) shows the state when k=1.48. For $k \geqslant 2.10$, the system settles into a turbulent state as k increases further. Figure 4(f) shows the state of the system when k=3.0.

C. Lyapunov exponents

In order to quantitatively examine the influence of time-delayed feedback when the arbitrary time delay τ and the proportionality constant k are varied, the Lyapunov exponents [21] are calculated based on chaotic analysis. The largest Lyapunov exponents calculated from the time series in Figs. 3 and 4 are shown in Figs. 5 and 6, respectively. In a chaotic system, the value of the largest Lyapunov exponent is positive; this value is higher for a more chaotic system. Further, this value is zero for a system with complete periodic oscillation. Figures 5(a)–5(e) correspond to the largest Lyapunov exponents calculated from the time series in Figs. 3(a)–3(e), respectively. In Fig. 5(a), the value of the largest Lyapunov exponent is 0.31. This implies that a limit cycle does not exhibit complete periodic oscillation but weak chaos although the oscillation appears periodic. In Fig. 5(b) and 5(d), the values of the largest Lyapunov exponents are 0.33 and 0.36, respectively, which are close to (a) 0.31. This is because the system is synchronized by time-delayed feedback. In Fig. 5(c), its value is 0.73, which is greater than or equal to two times that of Fig. 5(a). This is because the system is further disturbed by time-delayed feedback. In Fig. 5(e), its value is 0.42, which is marginally greater than in Fig. 5(a), 0.31. This is because the time-delayed feedback to the system causes it to transition to an unstable period-3 orbit. Figures 6(a)–6(f) correspond to the largest Lyapunov exponents that are calculated from the time series in Figs. 4(a)–4(f), respectively. In Fig. 6(a), the value of the largest Lyapunov exponent is 0.31, as shown in Fig. 5(a). In Figs. 6(b), 6(d), and 6(f), their values are 0.78, 0.93, and 0.71, respectively. On the other hand, in Figs. 6(c) and 6(e), their values are 0.23 and 0.27, respectively. In the former cases, the system is further disturbed by time-delayed feedback. In the latter cases, the system is stabilized because the values decrease to below that of Fig. 6(a), 0.31, due to synchronization. This particularly depends on whether the system becomes more orderly or disorderly with the choice of the proportionality constant k. Depending on τ and k, the motion associated with the NPR varies with time-delayed feedback. In certain regions, the system cannot be synchronized despite the application of time-delayed feedback. Therefore, τ and k should be carefully selected in order to achieve synchronization, or the system will be further disturbed by time-delayed feedback.

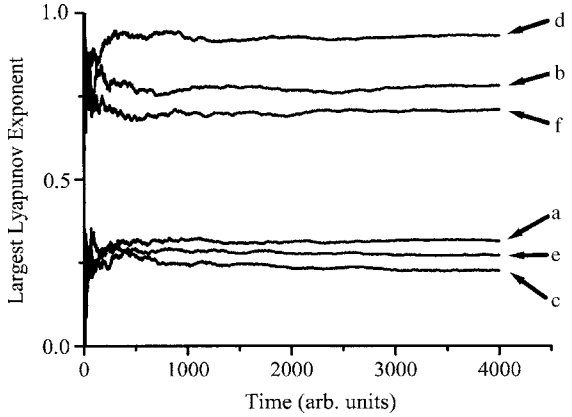

FIG. 6. The largest Lyapunov exponents calculated from the time series in Fig. 4. (a) 0.31 (before application), (b) 0.78 (k=0.64), (c) 0.23 (k=0.86), (d) 0.93 (k=1.30), (e) 0.27 (k=1.48), and (f) 0.71 (k=3.0).

IV. CONCLUSION

In conclusion, time-delayed feedback is applied to the motions associated with the NPR generated by the current-driven IAI and the dynamical behavior subject to delayed feedback is experimentally investigated. When a control parameter of the system, V_m, is increased, current-driven IAI is excited, and the system then demonstrates a nonlinear periodic orbit around V_m=40 V. The behavior of the system is investigated by changing τ and k when time-delayed feedback is applied to the motions associated with the NPR. Dynamical behavior such as intermittency and chaos is observed by changing τ and k. Furthermore, the largest Lyapunov exponents are calculated when, depending on τ and k, the motion associated with the NPR varies with time-delayed feedback. It is clarified that suitable values of τ and k should be chosen in order to achieve synchronization by using time-delayed feedback.

ACKNOWLEDGMENTS

The authors thank Dr. K. Itoh (NIFS), Dr. S.-I. Itoh (Kyushu University), Dr. T. Klinger (Max-Planck-Institute), and Dr. K. Fukushima (Kumamoto University) for their continuous encouragement and helpful advice. T.F. was supported by the Japan Society for the Promotion of Science.

[1] E. Ott, C. Grebogi, and J. A. Yorke, Phys. Rev. Lett. **64**, 1196 (1990).
[2] K. Pyragas, Phys. Lett. A **170**, 421 (1992).
[3] S. Bielawski, D. Derozier, and P. Glorieux, Phys. Rev. E **49**, R971 (1994).
[4] Th. Pierre, G. Bonhomme, and A. Atipo, Phys. Rev. Lett. **76**, 2290 (1996).
[5] P. Parmananda, R. Madrigal, M. Rivera, L. Nyikos, I. Z. Kiss, and V. Gaspar, Phys. Rev. E **59**, 5266 (1999).
[6] T. Fukuyama, R. Kozakov, H. Testrich, and C. Wilke, Phys. Rev. Lett. **96**, 024101 (2006).
[7] K. Taniguchi and Y. Kawai, Phys. Rev. Lett. **83**, 548 (1999).
[8] T. Fukuyama, K. Taniguchi, and Y. Kawai, Phys. Plasmas **9**, 1570 (2002).
[9] T. Fukuyama, H. Shirahama, and Y. Kawai, Phys. Plasmas **9**, 4525 (2002).
[10] R. J. Taylor, K. R. Mackenzie, and H. Ikezi, Rev. Sci. Instrum. **43**, 1675 (1972).
[11] K. Taniguchi, H. Kuwae, N. Hayashi, and Y. Kawai, Phys. Plasmas **5**, 401 (1998).
[12] M. Yamada and M. Raether, Phys. Fluids **18**, 361 (1975).
[13] K. Nishikawa and C.-S. Wu, Phys. Rev. Lett. **23**, 1020 (1969).
[14] D. B. Fenneman, M. Raether, and M. Yamada, Phys. Fluids **16**, 871 (1973).
[15] D.-I. Choi and W. Horton, Jr., Phys. Fluids **17**, 2048 (1974).
[16] H. Tanaca, A. Hirose, and M. Koganei, Phys. Rev. **161**, 94 (1967).
[17] Y. Kawai, Ch. Hollenstein, and M. Guyot, Phys. Fluids **21**, 970 (1978).
[18] W. Just, T. Bernard, M. Ostheimer, E. Reibold, and H. Benner, Phys. Rev. Lett. **78**, 203 (1997).
[19] W. Just, D. Reckwerth, J. Möckel, E. Reibold, and H. Benner, Phys. Rev. Lett. **81**, 562 (1998).
[20] P. Hövel and E. Schöll, Phys. Rev. E **72**, 046203 (2005).
[21] A. Wolf, J. B. Swift, H. L. Swinney, and J. A. Vastano, Physica D **16**, 285 (1985).